iScience

CellPress
OPEN ACCESS

Article

Oxygen-carrying sequential preservation mitigates liver grafts ischemia-reperfusion injury

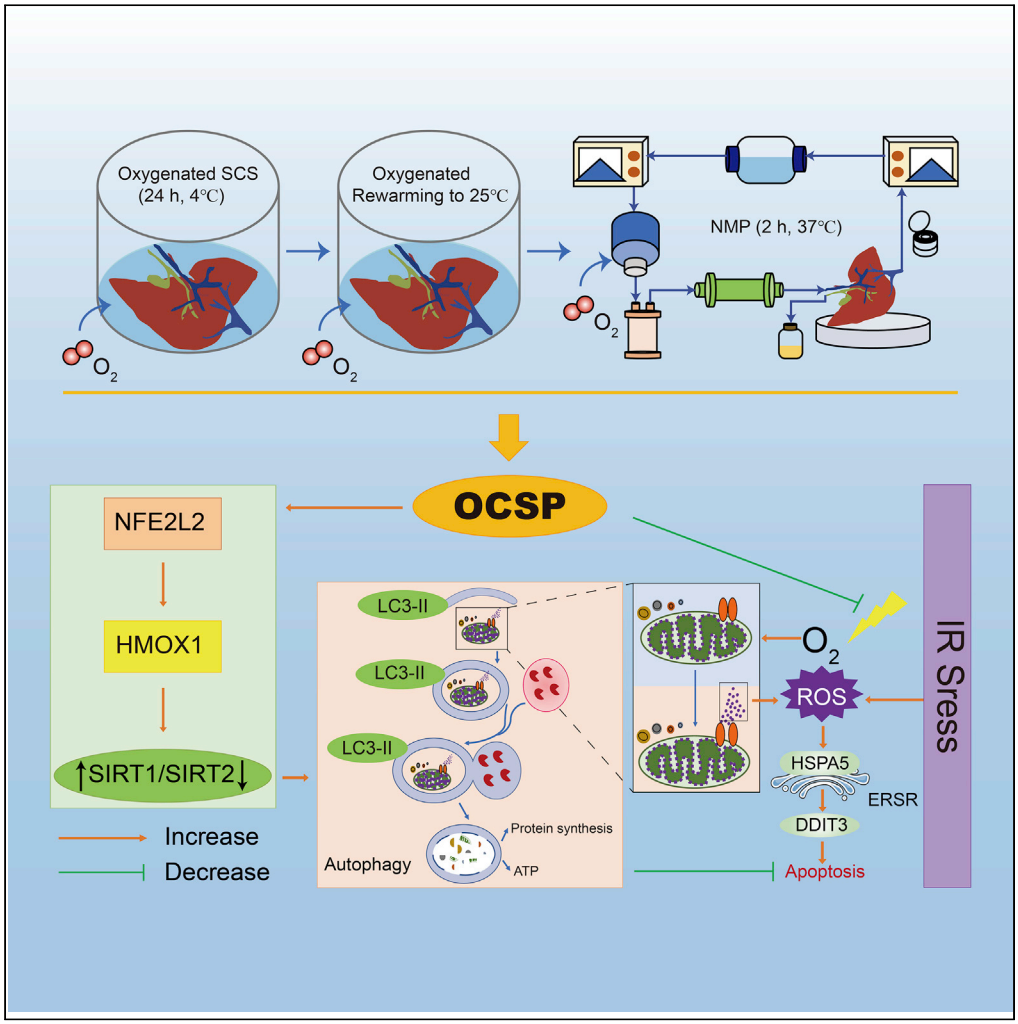

Jianbo Li, XiangJun Zha, Yan Kang, ..., Lujia Song, Chengdi Wang, Jiayin Yang

chengdi_wang@scu.edu.cn (C.W.)
doctoryjy@scu.edu.cn (J.Y.)

Highlights

OCSP provides an oxygen-enriched strategy to link SCS and NMP

A shared oxygen-dependent anti-IRI mechanism exists between preservation modes switch

Autophagy functions as an ERSR suppressor to counter liver graft's IRI under OCSP

Li et al., iScience 26, 105858
January 20, 2023
https://doi.org/10.1016/j.isci.2022.105858

iScience

CellPress
OPEN ACCESS

Article

Oxygen-carrying sequential preservation mitigates liver grafts ischemia-reperfusion injury

Jianbo Li,[1] XiangJun Zha,[2,3] Yan Kang,[1] Zhongwei Zhang,[1] Lvnan Yan,[3] Lujia Song,[4] Chengdi Wang,[4,*] and Jiayin Yang[3,5,*]

SUMMARY

Oxygen-dependent preservation has been proposed to protect liver grafts from ischemia-reperfusion injury (IRI), but its underlying mechanism remains elusive. Here, we proposed an oxygen-carrying sequential preservation (OCSP) method that combined oxygenated static cold storage (SCS) and normothermic mechanical perfusion. We demonstrated that OCSP, especially with high oxygen partial pressure level (500–650mmHg) during the oxygenated SCS phase, was associated with decreased IRI of liver grafts and improved rat survival after transplantation. A negative correlation between autophagy and endoplasmic reticulum stress response (ERSR) was found under OCSP and functional studies indicated OCSP suppressed ERSR-mediated cell apoptosis through autophagy activation. Further data showed that OCSP-induced autophagy activation and ERSR inhibition were oxygen-dependent. Finally, activated NFE2L2-HMOX1 signaling was found to induce autophagy under OCSP. Together, our findings indicate oxygen-dependent autophagy mitigates liver graft's IRI by ERSR suppression and modulates NFE2L2-HMOX1 signaling under OCSP, providing a theoretical basis for liver preservation using a composite-sequential mode.

INTRODUCTION

IRI is quite a challenge affecting the prognosis of liver transplantation. The organ-transfer attribute determines an inevitable ischemic stage during transplantation, especially a significant proportion of time for preservation. There are so far two well-developed preservation strategies: SCS and, lately, more advanced NMP.[1,2] Both have their pros and cons: SCS has a strong point in cost and ease of use, however, liver grafts submitted to SCS for more than 8 h are likely to suffer severe IRI following transplantation; NMP is efficient at sustaining energy metabolism and predicting liver function before transplantation while at the expense of high costs when used for long-term preservation. Theoretically, a sequential combination of these two classic approaches has a complementary advantage in liver preservation. However, the reasonably foreseeable IRI is likely to occur when cold ischemia of SCS switches into warm and oxygen-enriched perfusion of NMP. Now two problems need to be resolved for their better combination: One is in what situation the two approaches can be well organically integrated, and the other is whether there is a common anti-IRI mechanism under that specific situation. Unfortunately, there are currently no clear answers to these problems.

Recently, the continuous addition of oxygen (O_2) to the preservation solution has illustrated promising results regarding the quality improvement of liver grafts. Martins et al.[3] demonstrated that SCS with oxygenated University of Wisconsin (UW) solution through a double-layer method that pre-oxygenated perfluorocarbon in the lower layer continuously provided oxygen to the UW solution in the upper layer and the graft was placed at the interface between perfluorocarbon and UW solution-could improve rats' survival following transplantation of liver grafts from donation after circulatory death through decreased adenosine triphosphate (ATP) decay and better preservation of morphology after 4 h oxygenated SCS. Similarly, Asong-Fontem et al. added to the preservation solution IGL-1 a novel oxygen carrier called M101, which is isolated from extracellular hemoglobin extracted from a marine invertebrate and can carry 39 times oxygen molecules per structural unit as human hemoglobin, and rat steatotic livers were stored in such oxygenated solution at 4°C for 24 h, finding marked protection against IRI in terms of lower transaminases, glutamate dehydrogenase, lactate levels and reduced reactive oxygen species (ROS) at the end of

[1]Department of Critical Care Medicine, West China Hospital of Sichuan University, Chengdu 610041, China

[2]Department of Liver Surgery of West China Hospital and State Key Laboratory of Polymer Materials Engineering of Sichuan University, Chengdu610065, China

[3]Department of Liver Surgery and Liver Transplantation Center, West China Hospital of Sichuan University, Chengdu610041, China

[4]Department of Respiratory and Critical Care Medicine, Med-X Center for Manufacturing, Frontiers Science Center for Disease-related Molecular Network, West China Hospital, West China School of Medicine, Sichuan University, Chengdu, China

[5]Lead contact

*Correspondence: chengdi_wang@scu.edu.cn (C.W.), doctoryjy@scu.edu.cn (J.Y.)

https://doi.org/10.1016/j.isci.2022.105858

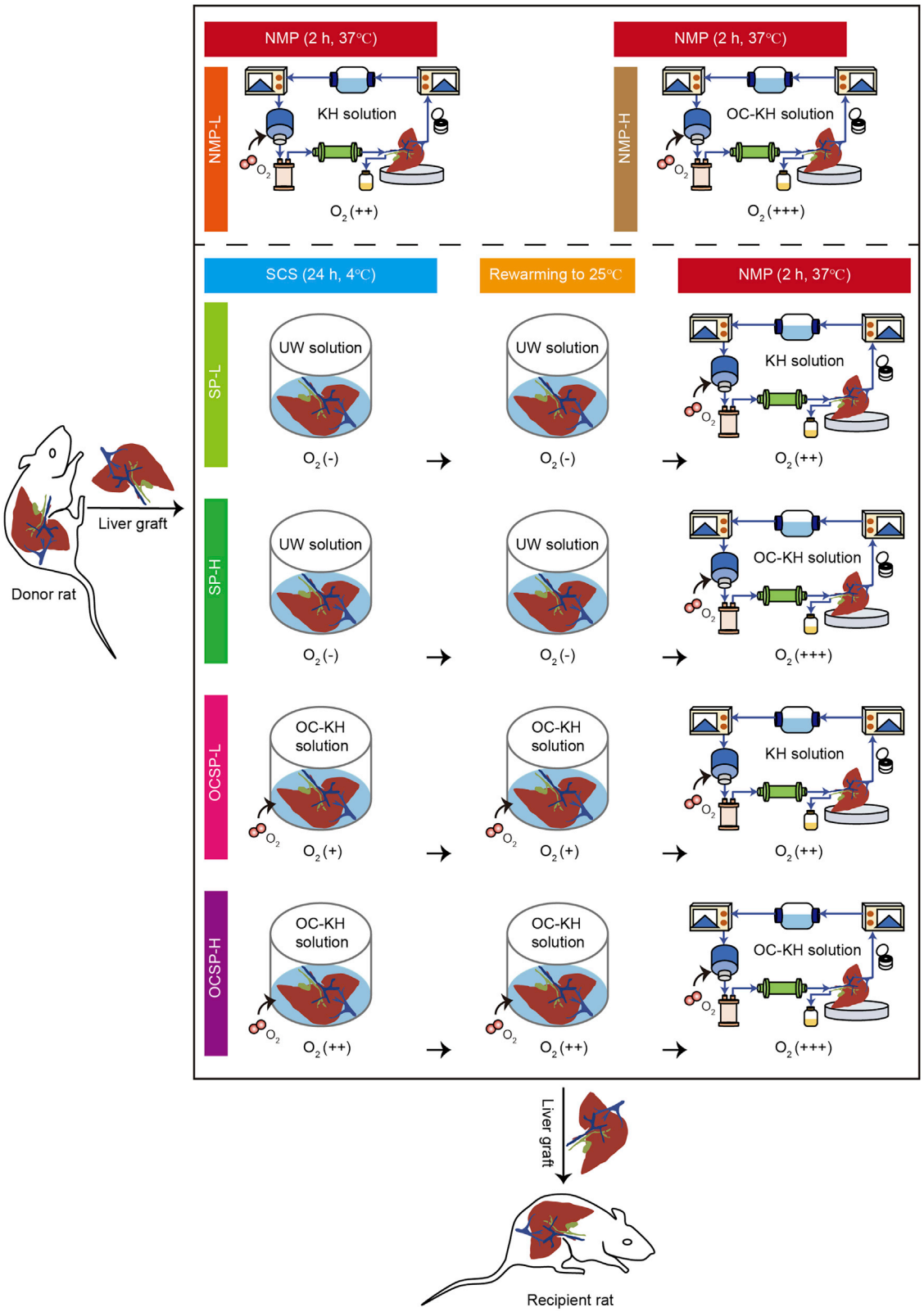
NMP (2 h, 37℃)
NMP-L
KH solution
O_2(++)
NMP (2 h, 37℃)
NMP-H
OC-KH solution
O_2(+++)
SCS (24 h, 4℃)
Rewarming to 25℃
NMP (2 h, 37℃)
SP-L
UW solution
O_2(-)
O_2(-)
KH solution
O_2(++)
SP-H
UW solution
O_2(-)
O_2(-)
OC-KH solution
O_2(+++)
OCSP-L
OC-KH solution
O_2(+)
O_2(+)
KH solution
O_2(++)
OCSP-H
OC-KH solution
O_2(++)
OC-KH solution
O_2(++)
OC-KH solution
O_2(+++)
Donor rat
Liver graft
Liver graft
Recipient rat

Figure 1. Experimental protocol for comparison of the effects of different PaO_2 levels on the rat liver preservation with NMP, SP, or OCSP method

"L" indicates relatively low PaO_2 levels and "H" indicates relatively high PaO_2 levels. "-" indicates $PaO_2 \leq 200$mmHg; "+" indicates 200mmHg$<PaO_2 \leq$ 500mmHg; "++" indicates 500mmHg$<PaO_2 \leq$650mmHg; "+++" indicates $PaO_2>$650mmHg.

reperfusion.[4] Before the occurrence of oxygenated SCS, oxygenated mechanical perfusion at various temperatures such as hypothermic oxygenated perfusion[5] and controlled oxygenated rewarming[6] has also displayed encouraging performance in improving liver quality against IRI. In addition, the clinical application of hypothermic oxygenated machine perfusion has very recently been proven in a randomized clinical trial, showing a lower risk of non-anastomotic biliary strictures following the transplantation of livers obtained from donors after circulatory death than conventional SCS.[7] All these findings evidenced the importance of the shared factor O_2 in the improvement of liver preservation.

Accordingly, we hypothesize that there is a shared anti-IRI mechanism behind the oxygen-enriched environment to link oxygenated SCS and oxygenated machine perfusion. Autophagy is a protective mechanism under cell stress associated with ERSR during liver SCS.[8] In recent years, studies have shown that autophagy plays an important role in the process of liver IRI.[9,10] In the pilot experiment, we found more autophagosomes presented in the liver tissue after oxygenated SCS; thus, we would like to explore whether autophagy plays a protective role against IRI when livers are submitted to oxygen-dependent preservation methods.

In emphasizing the importance of continuous oxygen-carrying, the concept/method of OCSP was introduced into the preservation of liver grafts for the first time. This OCSP method emphasizes how to switch between preservation modes, i.e. SCS and NMP, and intends to build a continuous oxygen-enriched environment to link oxygenated SCS and oxygenated machine perfusion (Figure 1). This study aimed to explore the optimal oxygen content to preserve liver grafts and disclose the potential oxygen-dependent anti-IRI mechanism with the OCSP method, providing a theoretical basis for the transformation of liver graft preservation from a single model to a composite sequential one.

RESULTSOC-KH solution is safe and effective for liver preservation

To evaluate the effect on the liver preservation of the modified KH solution which was added with polymers, we compared OC-KH solution and UW solution during the liver SCS phase and NMP phase respectively, and their cytotoxicity was evaluated by an IRI cell model (Figures S3 andS4). There was no significant difference between OC-KH solution and UW solution for liver preservation using SCS or NMP in terms of histopathological hematoxylin and eosin (HE) staining (Figures S3A and S3B), the expression level of HSP70 proteins as a cytoprotective factor (Figure S3C), terminal deoxynucleotidyl transferase-mediated dUTP nick end-labeling (TUNEL) fluorescent staining for cell apoptosis (Figures S3D and S3E), histopathological changes with the electron microscope (Figure S3F), transaminase release (Figures S3G and S3H), total bile outputs (Figure S3I) and malondialdehyde (MDA) content, as an indicator of lipid peroxidation (Figure S3J). OC-KH solution did not show significant cytotoxicity for LO_2 preservation in the IRI cell model when compared with UW solution with a similar apoptotic ratio (Figure S4B), cell integrity (Figure S4C), and cell viability (Figure S4D). Thus, OC-KH solution is effective and noncytotoxic for liver preservation.

PaO_2 level and ATP content are positively correlated during the oxygenated SCS phase of OCSP

To investigate the differences between different preservation processes regarding the association of PaO_2 levels in solution and ATP content of hepatic tissue, we separately plotted the PaO_2 levels and ATP concentration curves over time (Figure 2). When the liver was subjected to NMP directly without the SCS phase, there was no difference in ATP content between lower (around 600 mmHg) and higher (around 800 mmHg) PaO_2 levels. However, the PaO_2 levels significantly affected the liver ATP content during the SCS phase with the result that the higher the PaO_2 levels, the higher the ATP content. When no additional O_2 was fed into the solution during SCS, the liver ATP content decreased dramatically and led to no increase in ATP content even if O_2 was replenished during the sequential NMP. Thus, a high PaO_2 level is associated with high ATP content of hepatic tissue during the oxygenated SCS phase.

OCSP is effective against IRI of rat liver graft

To ascertain the effect of OCSP on the liver graft's IRI, cell apoptosis, lipid peroxidation, and liver function recovery were observed at the end of NMP and followed by orthotopic liver transplantation (Figure 3).

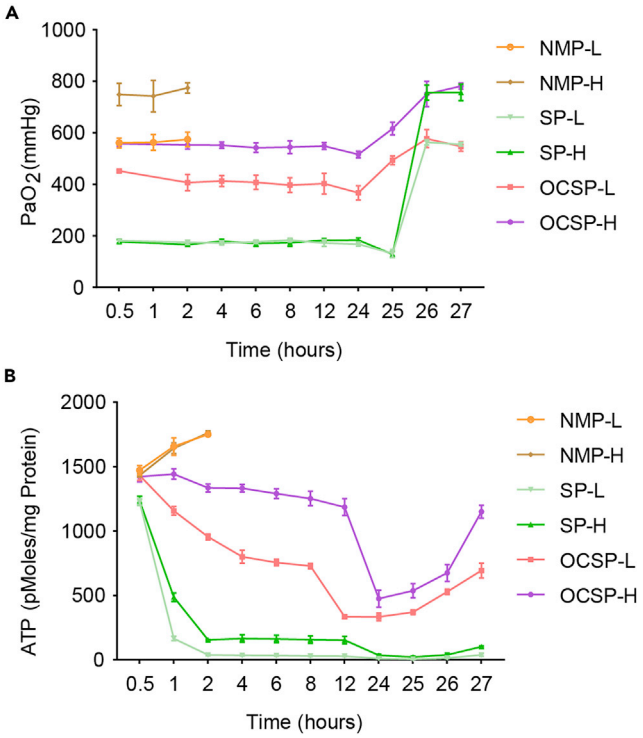

Figure 2. Associations between PaO_2 levels and ATP content of hepatic tissue during different preservation processes

(A) PaO_2 levels curves over time.

(B) ATP content curves over time.

(A and B) "L" indicates relatively low PaO_2 levels and "H" indicates relatively high PaO_2 levels. Data are represented as mean ± SD.

Compared to those in SP groups, livers in OCSP groups had a lower percentage of apoptosis cells in hepatic tissue (Figures 3A, 3B, 3G, and 3H). Regarding lipid peroxidation and liver function recovery, livers in OCSP with high PaO_2 levels during the SCS phase (OCSP-H) group exhibited a significant anti-IRI effect, with lower MDA formation, higher total bile outputs, and decreased transaminase levels (Figures 3C–3F). Regarding survival after transplantation, rats in control groups had the best outcome with a 50% of 50-day survival rate which was nearly 35% in the OCSP-H group (Figure 3I). All the rats in the OCSP-L died within 30 days and those in the SP-L or SP-H group died within 2 days after transplantation. Moreover, more activation of cytoprotective factors such as HSP70 and e-NOS proteins was observed in the OCSP-H group (Figures S5A and S5B). Taken together, OCSP, especially with high PaO_2 levels during the SCS phase, is associated with decreased IRI of rat liver grafts and improves survival after transplantation.

OCSP promotes autophagy but inhibits ERSR of rat liver graft

Compared to hypoxic SCS, we found more autophagosomes/autolysosomes presented in the liver tissue after oxygenated SCS (Figures S3F andS6); thus, we would like to explore whether autophagy plays a protective role against IRI for livers submitted to OCSP. Therefore, we conducted western blotting analysis for several molecular indicators of autophagy such as BECN1, ATG5, MAP1LC3B, and SQSTM1. We found that liver preservation with OCSP resulted in a marked increase in autophagic indicators when compared with other preservation processes as evidenced by the up-regulation of BECN1, ATG5, MAP1LC3B II as well as down-regulation of SQSTM1 (Figures 4A–4D).

Considering the potential relationship between autophagy and ERSR, we also investigated the expression of HSPA5 and DDIT3 as molecular indicators of ERSR. Western blotting analysis showed a marked decrease in HSPA5 and DDIT3 for livers preserved with OCSP (Figures 4E and 4F). Therefore, our results indicate a negative correlation between autophagy and ERSR in livers submitted to OCSP.

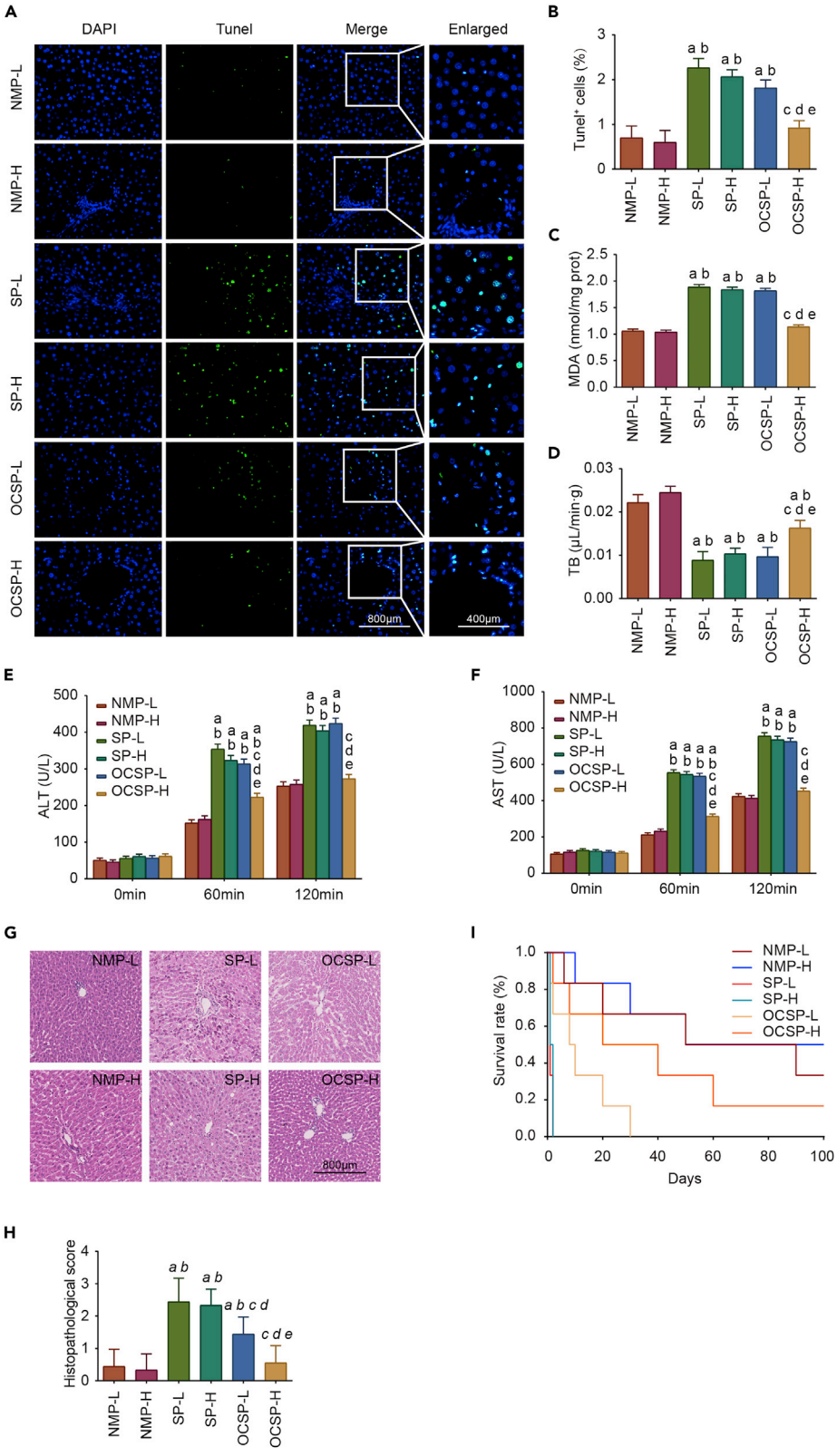
A
DAPI
Tunel
Merge
Enlarged
NMP-L
NMP-H
SP-L
SP-H
OCSP-L
OCSP-H
800μm
400μm
B
Tunel+ cells (%)
C
MDA (nmol/mg prot)
D
TB (μL/min·g)
E
ALT (U/L)
F
AST (U/L)
0min
60min
120min
G
H
Histopathological score
I
Survival rate (%)
Days

Figure 3. The effect of OCSP on IRI of rat liver graft and survival after transplantation

See also Figure S5.

(A) TUNEL fluorescent staining of hepatic tissue. The strong green fluorescence in the nucleus indicates cell apoptosis. Scale bar = 800 μm (original at left)/400 (enlarged at right).

(B) The percentage of apoptosis (%) of hepatic tissue according to TUNEL fluorescent staining. Data are represented as mean ± SD. p value was calculated using one-way ANOVA. $^{a}p < 0.05$ versus NMP-L, $^{b}p < 0.05$ versus NMP-H, $^{c}p < 0.05$ versus SP-L, $^{d}p < 0.05$ versus SP-H, $^{e}p < 0.05$ versus OCSP-L.

(C) MDA measurement of hepatic tissue at the end of 2 h of NMP phase. Data are represented as mean ± SD. p value was calculated using one-way ANOVA. $^{a}p < 0.05$ versus NMP-L, $^{b}p < 0.05$ versus NMP-H, $^{c}p < 0.05$ versus SP-L, $^{d}p < 0.05$ versus SP-H, $^{e}p < 0.05$ versus OCSP-L.

(D) TB outputs during 2 h of NMP phase. Data are represented as mean ± SD. p value was calculated using one-way ANOVA. $^{a}p < 0.05$ versus NMP-L, $^{b}p < 0.05$ versus NMP-H, $^{c}p < 0.05$ versus SP-L, $^{d}p < 0.05$ versus SP-H, $^{e}p < 0.05$ versus OCSP-L.

(E and F) Liver injury assessment according to ALT and AST levels in effluent perfusate at 1-h intervals during 2 h of NMP phase. Data are represented as mean ± SD. p value was calculated using one-way ANOVA. $^{a}p < 0.05$ versus NMP-L, $^{b}p < 0.05$ versus NMP-H, $^{c}p < 0.05$ versus SP-L, $^{d}p < 0.05$ versus SP-H, $^{e}p < 0.05$ versus OCSP-L.

(G) HE staining of liver grafts at the end of the different preservation processes. Scale bar = 800 μm.

(H) Histopathological score according to HE staining of liver grafts. Data are represented as mean ± SD. p value was calculated using one-way ANOVA. $^{a}p < 0.05$ versus NMP-L, $^{b}p < 0.05$ versus NMP-H, $^{c}p < 0.05$ versus SP-L, $^{d}p < 0.05$ versus SP-H, $^{e}p < 0.05$ versus OCSP-L.

(I) Survival curves of rats who underwent orthotopic liver transplantation.

(A–I) "L" indicates relatively low PaO_2 levels and "H" indicates relatively high PaO_2 levels.

OCSP suppresses ERSR-mediated cell apoptosis through autophagy activation

To determine whether the increase of MAP1LC3B because of OCSP is caused by the obstruction of autophagic flux, autophagy blocker chloroquine was used and western blot showed autophagic flux was enhanced under OCSP instead of being blocked (Figures 5A and 5B). Moreover, blockage of autophagic flux with chloroquine during OCSP indicated a positive correlation with enhanced ERSR exhibited as increased HSPA5 and DDIT3 protein levels (Figures 5A and 5B).

To further ascertain the relationship between autophagy and ERSR during OCSP against cell apoptosis, autophagy inhibitor 3-Methyladenine and ERSR agonist tunicamycin were respectively used before detecting related protein expression. Histopathological HE staining and TUNEL fluorescent staining were conducted for observation of the cell apoptosis in hepatic tissue (Figures 5C–5H). Autophagy inhibition induced a notable rise in HSPA5 and DDIT3 protein levels, and blockage of autophagic flux under OCSP also resulted in a significant ERSR activation (Figures 5C and 5D). Histopathological HE staining showed mild edema of hepatocytes but an obvious expansion of hepatic sinuses when autophagy inhibitor was used, which showed diffuse edema, eosinophilic degeneration of cytoplasm, and nuclear concentration in hepatocytes when ERSR agonist was used (Figures 5E and 5F). TUNEL fluorescent staining showed a marked increase of apoptosis cells in hepatic tissue both in the autophagy inhibition group and ERSR activation group (Figures 5G and 5H). Thus, our data indicate that OCSP activates autophagy to protect the liver from cell apoptosis caused by IRI-induced ERSR.

OCSP-induced autophagy activation and ERSR inhibition are oxygen dependent

To determine whether oxygen is the key for OCSP to activate autophagy and inhibit ERSR, we analyzed related proteins expression during the SCS phase of OCSP in three groups, without supplementary oxygen, with supplementary oxygen, or with supplementary oxygen and autophagy inhibitor (Figure 6). Autophagy and ERSR-related proteins with only supplementary autophagy inhibitor at different doses of 3-Methyladenine were also investigated and results showed that 3-Methyladenine at 30 mg/kg (as the dose used in Figure 6) during hypoxic SCS could more significantly inhibit autophagy and more significantly induce ERSR than at 15 mg/kg (Figure S7). Western blotting analysis showed activated autophagy in the oxygen supplement group evidenced by up-regulation of BECN1, ATG5, MAP1LC3B II, and down-regulation of SQSTM1, whereas ERSR was suppressed evidenced by down-regulation of HSPA5 and DDIT3. Inhibition of autophagy resulted in the reversion of HSPA5 and DDIT3 which were down-regulated in the oxygen supplement group (Figures 6E and 6F). By comparing the band density, the expression of MAP1LC3B II in the O_2(−)&3-Methyladenine (30 mg/kg) group (Figure S7) was lower and the increases of HSPA5 and DDIT3 were higher than those of O_2(+)&3-Methyladenine (30 mg/kg) group (Figure 6), indicating weaker autophagy and more severe ERSR during hypoxic SCS than oxygenated SCS. Therefore, hepatic autophagy activation and inhibition of ERSR are oxygen-dependent under OCSP.

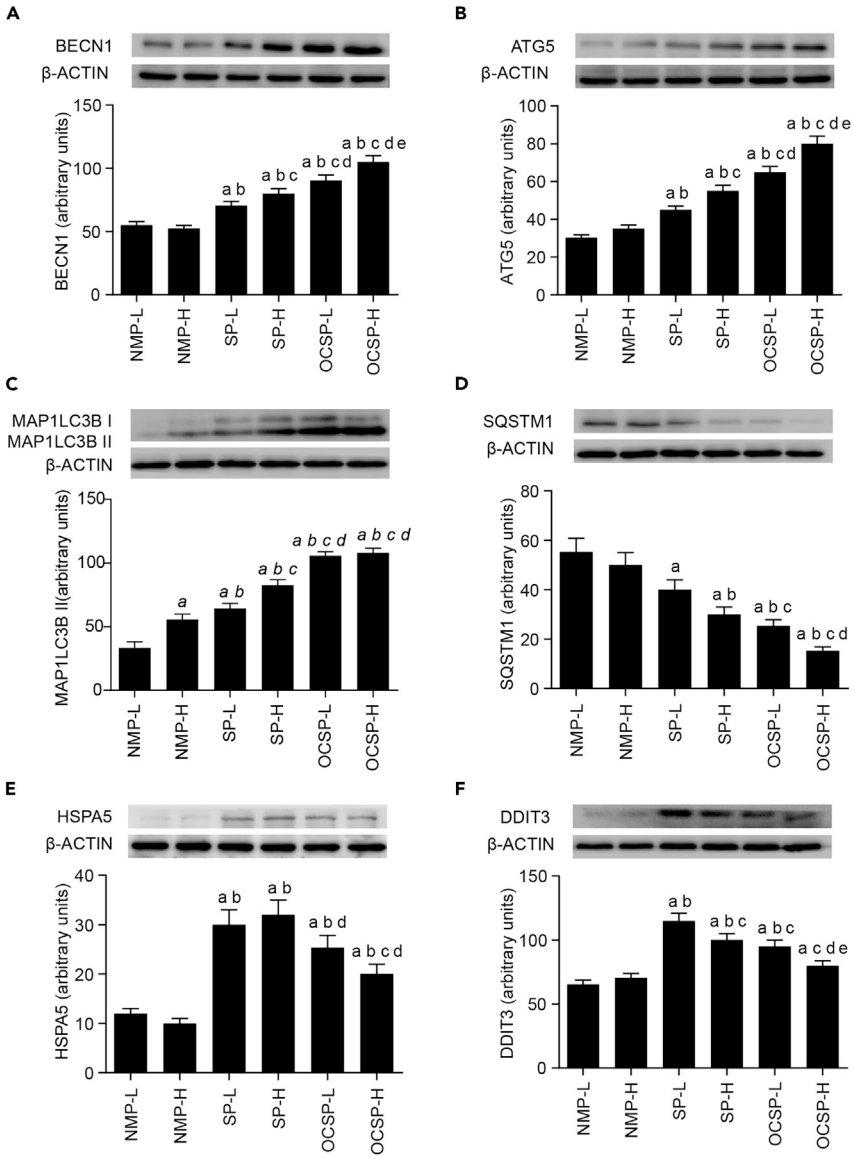

Figure 4. OCSP promotes autophagy but inhibits the expression of ERSR-related proteins

(A–F) Representative western blot at the top and densitometric analysis at the bottom of (A) BECN1, (B) ATG5, (C) MAP1LC3B II, (D) SQSTM1, (E) HSPA5, and (F) DDIT3. "L" indicates relatively low PaO_2 levels and "H" indicates relatively high PaO_2 levels. Data are represented as mean ± SD. p value was calculated using one-way ANOVA. $^{a}p < 0.05$ versus NMP-L, $^{b}p < 0.05$ versus NMP-H, $^{c}p < 0.05$ versus SP-L, $^{d}p < 0.05$ versus SP-H, $^{e}p < 0.05$ versus OCSP-L.

OCSP activates NFE2L2-HMOX1 signaling to induce autophagy

To further explore how autophagy is induced during OCSP-H, we investigated NFE2L2-HMOX1 signaling which was reported to be activated as a cytoprotective response both during liver SCS and NMP,[11,12] using HMOX1 inhibitor or not (Figure 7). We found the NFE2L2-HMOX1 signaling was markedly increased during OCSP evidenced by enhanced immunofluorescence staining of HMOX1 and increased protein levels of HMOX1 and nucleus NFE2L2 (Figures 7A–7C). Compared with livers in the control group (SP-H), the western blotting analysis showed inhibition of HMOX1 in the OCSP-H group led to decreased autophagy activation (decreased MAP1LC3B II), increased ERSR (upregulation of DDIT3) and increased apoptosis (increased Cleaved-caspase 3) (Figures 7B and 7C). In addition, SIRT1 and SIRT2 manifesting as an inverse relationship during OCSP-H seemed to mediate autophagy activated by NFE2L2-HMOX1 signaling (Figures 7B and 7C). Taken together, these results indicate that OCSP induces autophagy by activating NFE2L2-HMOX1 signaling.

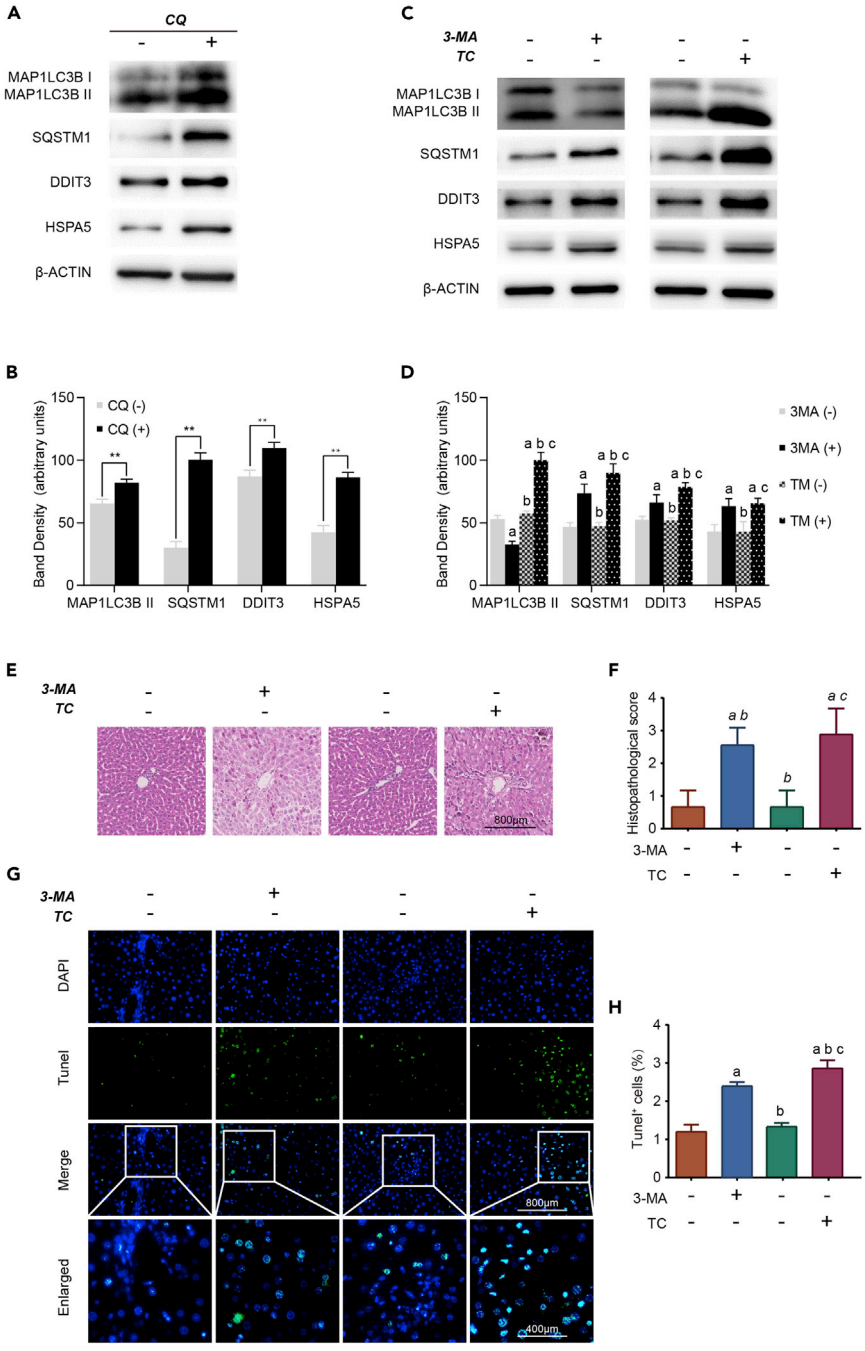

Figure 5. Liver autophagy activation by OCSP with high PaO_2 levels suppresses ERSR-mediated cell apoptosis

(A) Representative western blot of autophagy and ERSR-related proteins when autophagic flux was blocked with chloroquine (CQ).

(B) Densitometric analysis according to western blot results in Figure 5A. Data are represented as mean ± SD. p value was calculated using Student's *t* test. *p <0.05, **p <0.01.

(C) Representative western blot of autophagy and ERSR-related proteins when autophagy was inhibited with 3-Methyladenine or ERSR was enhanced with tunicamycin (TC).

(D) Densitometric analysis according to western blot results in Figure 5C. Data are represented as mean ± SD. p value was calculated using one-way ANOVA. [a]p < 0.05 versus 3-MA (–), [b]p < 0.05 versus 3-MA (+), [c]p < 0.05 versus TC (–).

(E) HE staining of hepatic tissue. Scale bar = 800 μm.

Figure 5. *Continued*

(F) Histopathological score according to HE staining of hepatic tissue. Data are represented as mean ± SD. p value was calculated using one-way ANOVA. [a]$p < 0.05$ versus 3-MA (−), [b]$p < 0.05$ versus 3-MA (+), [c]$p < 0.05$ versus TC (−).

(G) TUNEL fluorescent staining of hepatic tissue. The strong green fluorescence in the nucleus indicates cell apoptosis. Scale bar = 800 μm (original at upper)/400 (enlarged at lower).

(H) The percentage of apoptosis (%) of hepatic tissue according to TUNEL fluorescent staining. Data are represented as mean ± SD. p value was calculated using one-way ANOVA. [a]$p < 0.05$ versus 3-MA (−), [b]$p < 0.05$ versus 3-MA (+), [c]$p < 0.05$ versus TC (−).

(A and B) CQ (+), rats were intraperitoneally injected (50 mg/kg) with autophagy blocker chloroquine 2 h before OCSP-H. (C–H) 3-MA (+), rats were intraperitoneally injected (30 mg/kg) with autophagy inhibitor 3-Methyladenine 1 h before OCSP-H; TC (+), rats were intraperitoneally injected (0.5 mg/kg) with the ERSR agonist tunicamycin 1 h before OCSP-H.

DISCUSSION

In liver transplantation, a series of organ preservation techniques have developed around how to minimize graft's IRI. More advanced technical concepts such as supercooling liver preservation (SLP) and ischemia-free organ transplantation (IFOT) have also been proposed.[13–15] Without exception, these preservation techniques or concepts are inseparable from the corresponding solutions containing different bioactive additives to optimize the preservation quality, such as antioxidants (glutathione) in the UW solution for SCS, oxygen carriers (red blood cells or hemoglobin) in perfusion solutions for NMP, cryoprotective components (trehalose and glycerol) added to UW solution for SLP,[13] and even whole blood, if considered as a special solution containing all the ingredients needed for body metabolism, for IFOT.[14] The oxygenation preservation technique can be seen as the extension of NMP from normothermic temperature to various temperatures. To adapt to this technique, it becomes a necessity to develop oxygen carriers that meet the requirements of oxygen release rates at different temperatures. We developed a thermosensitive polymer material to act as this oxygen carrier. Although intermittent oxygen supplementation is still required to achieve a continuous oxygenation process at present, the use of this oxygen carrier in our study demonstrates the feasibility of achieving temperature-dependent control of PaO_2 level in liver preservation solutions.

Oxygenation preservation of liver grafts is based on the idea that hepatocytes can benefit from energy substrates and O_2 for ongoing liver metabolism, although it is dramatically reduced under hypothermia. The O_2 can help mitochondria switch from a high-flux stage which causes the release of ROS during reperfusion, to a low-flux electron transfer stage at the point of approximately 1.5 h following hypothermic oxygenated perfusion.[16] Theoretically, low temperature corresponds to reduced tissue metabolic rate and low O_2 demand. However, the additional O_2 delivery is necessary at normal body temperature, making the addition of red blood cells or an artificial oxygen carrier becomes a natural essential in common knowledge. Bral et al.[17] investigated the minimal hemoglobin level necessary for liver NMP through an experimental porcine normothermic ex situ liver perfusion model. They found a hemoglobin concentration of between 30 and 20 g/L could achieve the goal of assuring optimal liver graft function instead of the normal physiological range.[17] That means as long as the O_2 content in the preservation solution reaches 1/4 to 1/6 of the whole blood, it can fully meet the metabolic needs of the liver at normal temperature. This finding seems to explain the rationality of Boehnert's conclusion that 8 h of acellular NMP could still protect the liver and bile duct from the damage of pig livers retrieved after cardiac death.[18] In Boehnert's study, the perfusate was an oxygenated Steen solution, a buffered extracellular solution containing dextran and albumin as the provider for colloid osmotic pressure, which could satisfy the liver average O_2 consumption of 430 mmHg PaO_2 between pre and post-liver during acellular NMP.[18] Consistent with these results, our data confirm that the increase of PaO_2 in the NMP phase cannot further improve the preservation quality of the liver. However, in line with the previous finds,[3] the high PaO_2 in the SCS phase is related to the maintenance of high-level ATP content and can continue to affect the recovery of ATP in the subsequent NMP process. With the increase in temperature, ATP consumption increases faster than synthesis, especially during NMP storage which leads to ATP loss in the initial short time. Although at the end of 2 h NMP were ATP levels still lower than *in vivo* liver, ATP growth of the high PaO_2 group indicated a trend for energetic recovery as shown by the slope of the ATP curve during the NMP stage in Figure 2. Therefore, we believe that what is necessary is not to increase the absolute amount of ATP but to gradually restore the synthesis capacity of ATP, especially after long-term storage calling for a sequential and gentle process to allow for adapting. This is also the core concept of OCSP.

IRI is an acute injury often suffered by blood flow recanalization after cold preserved livers. It is one of the main sources of transplanted liver injury, which is often simulated using *in vitro* NMP model or orthotopic

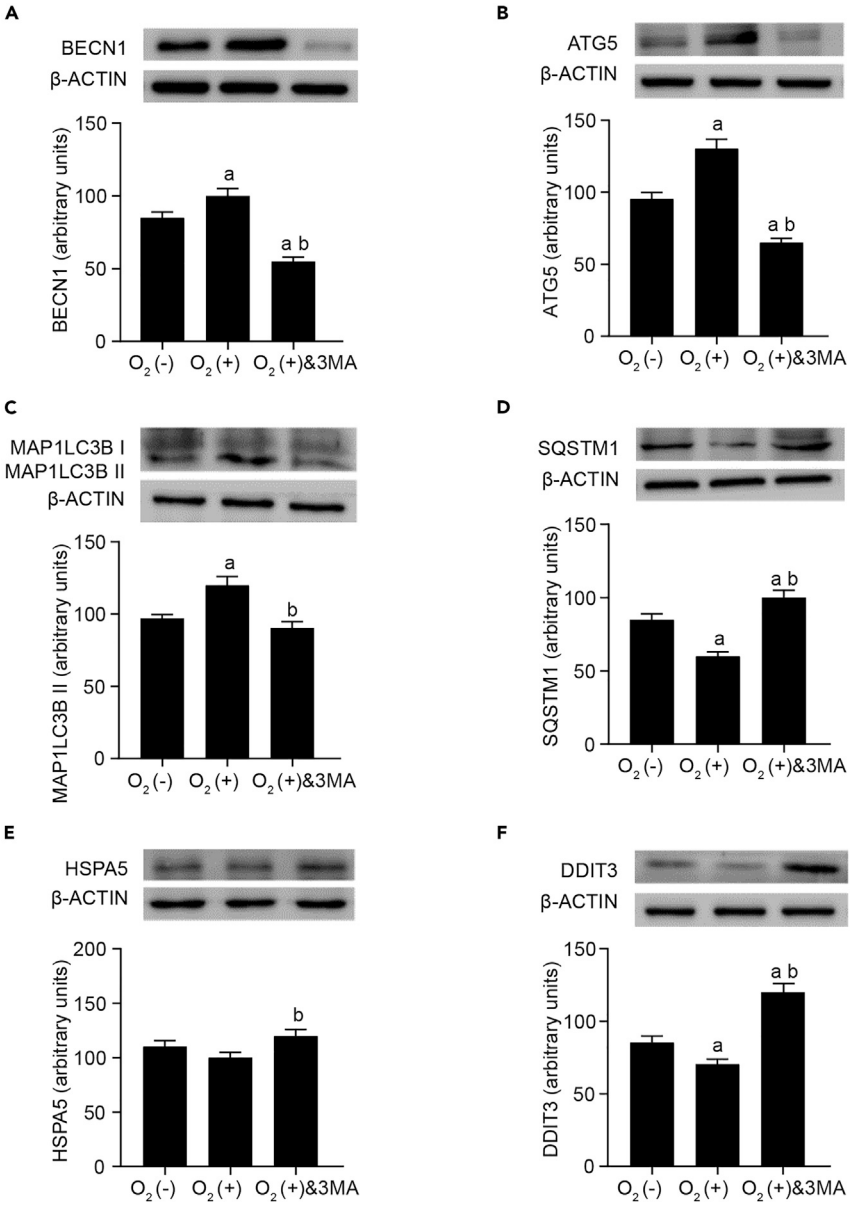

Figure 6. Hepatic autophagy activation and inhibition of ERSR were oxygen-dependent during SCS with the OCSP method

(A–F) Representative western blot at the top and densitometric analysis at the bottom of (A) BECN1, (B) ATG5, (C) MAP1LC3B II, (D) SQSTM1, (E) HSPA5, and (F) DDIT3. O_2 (+), oxygen was intermittently fed into OC-KH solution from outside to obtain a medium-grade level of oxygen partial pressure (PaO_2); O_2 (−), no oxygen was intermittently fed into OC-KH solution from outside; 3 MA (+), rats were intraperitoneally injected (30 mg/kg) with autophagy inhibitor 3-Methyladenine 1 h before SCS. Data are represented as mean ± SD. p value was calculated using one-way ANOVA. [a]$p < 0.05$ versus O_2 (−), [b]$p < 0.05$ versus O_2 (+). See also Figures S6 and S7.

liver transplantation model in animal experiments. Our data indicate OCSP with high PaO_2 level during the SCS phase significantly decreased the IRI of rat liver grafts evidenced by reduced cell apoptosis and rapid liver function recovery during the NMP phase, and improved rats' survival after orthotopic liver transplantation. To further explore the potential molecular mechanism behind OCSP, we investigated cell stress-related biological effects including autophagy and ERSR. Autophagy has contradictory functions according to specific cell events and plays an important role in the life-or-death decision for cellular stress response. In liver warm IRI, autophagy acts as a compensatory mechanism to balance ATP deprivation during the

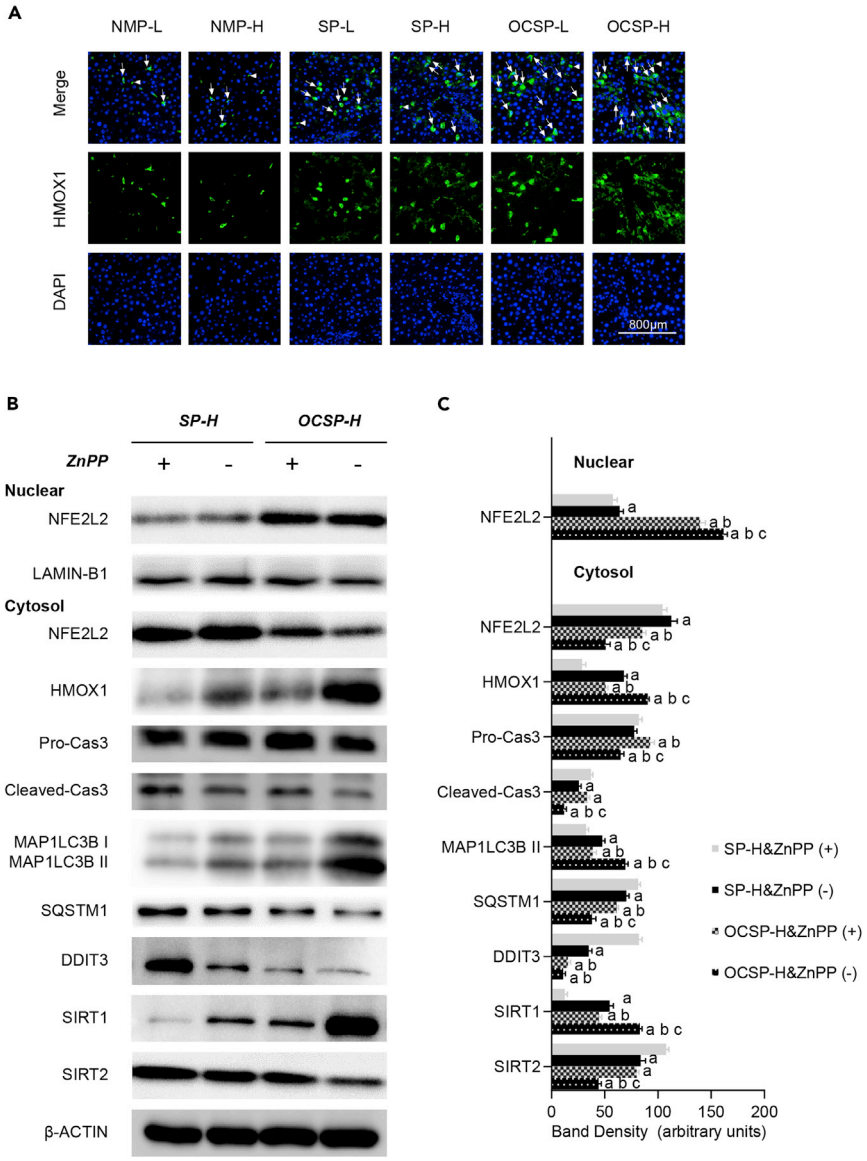

Figure 7. Activation of NFE2L2-HMOX1 signaling in hepatic tissue was closely related to autophagy activation by OCSP with high PaO_2 levels

(A) The expression of HMOX1 protein in hepatic tissue cells after different preservation processes. "L" indicates relatively low PaO_2 levels and "H" indicates relatively high PaO_2 levels. Arrows indicate hepatocytes and triangles indicate sinusoidal endothelial cells. Scale bar = 800 μm.

(B) Representative western blot of nucleus NFE2L2, and cytosolic NFE2L2, HMOX1, Pro/Cleaved-caspase 3, MAP1LC3B II, DDIT3, SIRT1/2. "H" indicates relatively high PaO_2 levels.

(C) Densitometric analysis according to western blot results. Data are represented as mean ± SD. p value was calculated using one-way ANOVA. $^{a}p < 0.05$ versus SP-H&ZnPP (+), $^{b}p < 0.05$ versus SP-H&ZnPP (–), $^{c}p < 0.05$ versus OCSP-H&ZnPP (+).

(B and C) ZnPP (+), rats were intraperitoneally injected (30 mg/kg) with HMOX1 inhibitor zinc protoporphyrin (ZnPP) 2 h before SP-H or OCSP-H.

ischemic phase; however, sustained or overactivated autophagy can lead to cell death during the reperfusion phase. In the context of liver transplantation, autophagy is generally shown to limit liver IRI, because ATP consumption in cold ischemia is not as intense as in warm ischemia.[9,10] Thus, if autophagy is maintained at a controlled level, it plays a lasting cytoprotective role. This protective process is likely related to mitophagy, which is involved in mitochondrial quality control by increasing the removal of damaged

mitochondria and which is from the mitochondrial respiratory chain, a major source of superoxide which in turn forms hydrogen peroxide and other destructive ROS.[19,20] ERSR is an adaptive response to misfolded proteins, but an excessive ERSR always triggers inflammatory responses and apoptosis. Experimental evidence suggests that strong ERSR is the initiator of the cell death mechanism during IRI, and the addition of unfolded protein response inhibitors to liver preservation solution could significantly attenuate ERSR-mediated apoptosis after liver graft reperfusion.[21,22] It should be pointed out that ERSR can cause apoptosis and autophagy at the same time, whereas autophagy can also alleviate ERSR by endogenously replenishing ATP, removing damaged mitochondria, and limiting ROS release. Both of them could exist in the donor's liver IRI and exhibit opposite biological effects,[8,23] however, the specific interaction mechanism between them has not been fully studied. Our data demonstrate that ERSR-mediated cell apoptosis during OCSP is suppressed through autophagy activation whereas this apoptosis is aggravated because of ERSR activation as a result of significant blockage of autophagic flux which is oxygen-dependent.

Livers preserved with SCS or NMP may have a common anti-IRI mechanism. In the early stage of ischemic injury, some highly conserved endogenous protective genes are induced to express, and they are regulated by the transcription factor NFE2L2. NFE2L2 is a basic leucine zipper protein with a cap-*n*-collar structure. Under physiological conditions, NFE2L2 binds to the cytoplasmic inhibitor Kelch-like ECH-associated protein 1 (KEAP1) and is degraded by ubiquitination under the action of E3 ubiquitin ligase, thereby avoiding translocation into the nucleus to generate signal transduction effect.[24,25] The activation of NFE2L2 plays an important role in improving the IRI of the donor's liver, as follows: (1) KEAP1-NFE2L2 complex can alleviate the reperfusion injury of the mouse donor liver after 20 h of SCS followed by orthotopic transplantation[11]; (2) In discarded human donor livers treated with NMP for 6 h, those with high expression of NFE2L2 significantly reduced hepatic enzyme release and increased lactate clearance.[12] *Hmox1* is the target gene of NFE2L2, and it may be the most promising therapeutic target for relieving liver grafts IRI. The downstream protective mechanisms initiated by HMOX1 mainly include[26,27]: (1) The classical protective function is that HMOX1 decomposes heme into biliverdin and carbon monoxide, of which the former acts anti-inflammatory effect by scavenging ROS and the latter exerts an anti-apoptotic effect by activating the mitogen-activated protein kinase pathway; (2) The non-classical macrophage pathway is that HMOX1 selectively reduces the infiltration of pro-inflammatory macrophages and inhibits the expression of CASPASE-3 to protect from cell apoptosis. Recently, Rao et al.[28] reported that the activation of the NFE2L2-HMOX pathway by the NFE2L2 agonist Oltipraz could activate the anti-inflammatory function of transcription activator 3 to prevent liver IRI. In our study, NFE2L2-HMOX1 signaling is activated with the OCSP method to induce autophagy during liver preservation. Furthermore, we found that HMOX1 correlated with SIRT1 and SIRT2. SIRT1, a member of the sirtuin family, is mainly located in the nucleus and can activate autophagy through a variety of signaling pathways. SIRT2 is the only sirtuin member which is found to be mainly located in the cytoplasm. Compared with SIRT1, the existing literature reported less on the biological role of SIRT2. Previous studies have reported inconsistent results on the relationship between SIRT2 and autophagy: on the one hand, decreased SIRT2 expression resulted in increased autophagy levels in human colon cancer cells HCT116; on the other hand, absence of autophagy was observed in *Sirt2−/−* mice.[29] Our data showed that the expression of SIRT1 in rat liver grafts was increased by OCSP, whereas the expression of SIRT2 was decreased; inhibition of HMOX1 resulted in the down-regulation of SIRT1 expression and up-regulation of SIRT2 expression.

Significance

In summary, our findings indicate that oxygen-dependent autophagy functions as an ERSR suppressor to counter liver graft's IRI by OCSP-stimulated NFE2L2-HMOX1 signaling. Oxygen-dependent autophagy provides a theoretical basis for the transformation of liver preservation from a single model to a composite-sequential mode.

Limitations of the study

In this study, we developed a novel liver preservation method to mitigate liver graft IRI and highlighted the importance of continuous oxygen-carrying in the cold, while warming up and during NMP. Although we found a shared anti-IRI mechanism behind the oxygen-enriched environment to link oxygenated SCS and NMP, we were not sure whether this mechanism was also applicable to switching between other oxygen-carrying modes, such as between hypothermic oxygenated perfusion and NMP. Furthermore, longer duration and more time points of liver sampling and molecular detection for *ex vivo* reperfusion may be

conducive to depicting molecular change trajectory and providing the basis for personalized liver preservation, but this requires more research input in the future.

STAR★METHODS

Detailed methods are provided in the online version of this paper and include the following:

- KEY RESOURCES TABLE
- RESOURCE AVAILABILITY
  - Lead contact
  - Materials availability
  - Data and code availability
- EXPERIMENTAL MODEL AND SUBJECT DETAILS
  - Animals
  - Cell lines
- METHOD DETAILS
  - Development of the thermal-regulated oxygen-carrying solution
  - OCSP method
  - Experimental protocols
  - Orthotopic liver transplantation model
  - *In vitro* IRI cell model
  - Biochemical determinations
  - Immunohistochemistry
  - Western blots analysis
  - Histology
  - Electron microscopy
  - Terminal deoxynucleotidyl transferase-mediated dUTP nick end-labeling (TUNEL) assay
  - ATP assay
- QUANTIFICATION AND STATISTICAL ANALYSIS
- ADDITIONAL RESOURCES

SUPPLEMENTAL INFORMATION

Supplemental information can be found online at https://doi.org/10.1016/j.isci.2022.105858.

ACKNOWLEDGMENTS

We gratefully acknowledge the support from the Sichuan Province Science and Technology Department Project (no. 2021YJ0448) (J.B.L), the 1.3.5 Project for Disciplines of Excellence, West China Hospital, Sichuan University (no. ZY2017308) (J.Y.Y.), Chinese Foundation for Hepatitis Prevention and Control-TianQing Liver Disease Research Fund Subject (no. TQGB20210186) (J.B.L) and Post-Doctoral Research Fund, West China Hospital, Sichuan University (no. 2020HXBH181) (J.B.L).

AUTHOR CONTRIBUTIONS

J.B.L., C.D.W., and J.Y.Y. designed the study and interpreted the data. J.B.L. and X.J.Z. performed the experiments and created figures. J.B.L. and C.D.W. wrote the main manuscript. J.B.L., X.J.Z., Y.K., and Z.W.Z. created the methods and figure legends. L.N.Y, L.J.S., W.Y., and J.Y.Y. edited the manuscript.

DECLARATION OF INTERESTS

The authors declare no competing interests.

INCLUSION AND DIVERSITY

We support the inclusive, diverse, and equitable conduct of research.

Received: July 18, 2022
Revised: November 1, 2022
Accepted: December 18, 2022
Published: January 20, 2023

REFERENCES

1. Nasralla, D., Coussios, C.C., Mergental, H., Akhtar, M.Z., Butler, A.J., Ceresa, C.D.L., Chiocchia, V., Dutton, S.J., García-Valdecasas, J.C., Heaton, N., et al. (2018). A randomized trial of normothermic preservation in liver transplantation. Nature *557*, 50–56. https://doi.org/10.1038/s41586-018-0047-9.

2. Burra, P., Zanetto, A., Russo, F.P., and Germani, G. (2018). Organ preservation in liver transplantation. Semin. Liver Dis. *38*, 260–269. https://doi.org/10.1055/s-0038-1666840.

3. Martins, P.N., Berendsen, T.A., Yeh, H., Bruinsma, B.G., Izamis, M.L., Op den Dries, S., Gillooly, A.R., Porte, R., Yarmush, M.L., Uygun, K., and Markmann, J.F. (2019). Oxygenated UW solution decreases ATP decay and improves survival after transplantation of DCD liver grafts. Transplantation *103*, 363–370. https://doi.org/10.1097/tp.0000000000002530.

4. Asong-Fontem, N., Panisello-Rosello, A., Lopez, A., Imai, K., Zal, F., Delpy, E., Rosello-Catafau, J., and Adam, R. (2021). A novel oxygen carrier (M101) attenuates ischemia-reperfusion injuries during static cold storage in steatotic livers. Int. J. Mol. Sci. *22*, 8542. https://doi.org/10.3390/ijms22168542.

5. Dutkowski, P., Furrer, K., Tian, Y., Graf, R., and Clavien, P.A. (2006). Novel short-term hypothermic oxygenated perfusion (HOPE) system prevents injury in rat liver graft from non-heart beating donor. Ann. Surg. *244*, 968–976. https://doi.org/10.1097/01.sla.0000247056.85590.6b.

6. Minor, T., Efferz, P., Fox, M., Wohlschlaeger, J., and Lüer, B. (2013). Controlled oxygenated rewarming of cold stored liver grafts by thermally graduated machine perfusion prior to reperfusion. Am. J. Transplant. *13*, 1450–1460. https://doi.org/10.1111/ajt.12235.

7. van Rijn, R., Schurink, I.J., de Vries, Y., van den Berg, A.P., Cortes Cerisuelo, M., Darwish Murad, S., Erdmann, J.I., Gilbo, N., de Haas, R.J., Heaton, N., et al. (2021). Hypothermic machine perfusion in liver transplantation - a randomized trial. N. Engl. J. Med. *384*, 1391–1401. https://doi.org/10.1056/NEJMoa2031532.

8. Zaouali, M.A., Boncompagni, E., Reiter, R.J., Bejaoui, M., Freitas, I., Pantazi, E., Folch-Puy, E., Abdennebi, H.B., Garcia-Gil, F.A., and Roselló-Catafau, J. (2013). AMPK involvement in endoplasmic reticulum stress and autophagy modulation after fatty liver graft preservation: a role for melatonin and trimetazidine cocktail. J. Pineal Res. *55*, 65–78. https://doi.org/10.1111/jpi.12051.

9. Wang, J.H., Ahn, I.S., Fischer, T.D., Byeon, J.I., Dunn, W.A., Jr., Behrns, K.E., Leeuwenburgh, C., and Kim, J.S. (2011). Autophagy suppresses age-dependent ischemia and reperfusion injury in livers of mice. Gastroenterology *141*, 2188–2199.e6. https://doi.org/10.1053/j.gastro.2011.08.005.

10. Schneider, J.L., and Cuervo, A.M. (2014). Liver autophagy: much more than just taking out the trash. Nat. Rev. Gastroenterol. Hepatol. *11*, 187–200. https://doi.org/10.1038/nrgastro.2013.211.

11. Ke, B., Shen, X.D., Zhang, Y., Ji, H., Gao, F., Yue, S., Kamo, N., Zhai, Y., Yamamoto, M., Busuttil, R.W., and Kupiec-Weglinski, J.W. (2013). KEAP1-NRF2 complex in ischemia-induced hepatocellular damage of mouse liver transplants. J. Hepatol. *59*, 1200–1207. https://doi.org/10.1016/j.jhep.2013.07.016.

12. Ahmed, O., Xu, M., Zhou, F., Wein, A.N., Upadhya, G.A., Ye, L., Wong, B.W., Lin, Y., O'Farrelly, C., and Chapman, W.C. (2022). NRF2 assessment in discarded liver allografts: a role in allograft function and salvage. Am. J. Transplant. *22*, 58–70. https://doi.org/10.1111/ajt.16789.

13. de Vries, R.J., Tessier, S.N., Banik, P.D., Nagpal, S., Cronin, S.E.J., Ozer, S., Hafiz, E.O.A., van Gulik, T.M., Yarmush, M.L., Markmann, J.F., et al. (2019). Supercooling extends preservation time of human livers. Nat. Biotechnol. *37*, 1131–1136. https://doi.org/10.1038/s41587-019-0223-y.

14. He, X., Guo, Z., Zhao, Q., Ju, W., Wang, D., Wu, L., Yang, L., Ji, F., Tang, Y., Zhang, Z., et al. (2018). The first case of ischemia-free organ transplantation in humans: a proof of concept. Am. J. Transplant. *18*, 737–744. https://doi.org/10.1111/ajt.14583.

15. Bruinsma, B.G., Berendsen, T.A., Izamis, M.L., Yeh, H., Yarmush, M.L., and Uygun, K. (2015). Supercooling preservation and transplantation of the rat liver. Nat. Protoc. *10*, 484–494. https://doi.org/10.1038/nprot.2015.011.

16. Bodewes, S.B., van Leeuwen, O.B., Thorne, A.M., Lascaris, B., Ubbink, R., Lisman, T., Monbaliu, D., De Meijer, V.E., Nijsten, M.W.N., and Porte, R.J. (2020). Oxygen transport during ex situ machine perfusion of donor livers using red blood cells or artificial oxygen carriers. Int. J. Mol. Sci. *22*, 235. https://doi.org/10.3390/ijms22010235.

17. Bral, M., Gala-Lopez, B., Thiesen, A., Hatami, S., Bigam, D.L., Freed, D.M., and James Shapiro, A.M. (2018). Determination of minimal hemoglobin level necessary for normothermic porcine ex situ liver perfusion. Transplantation *102*, 1284–1292. https://doi.org/10.1097/tp.0000000000002272.

18. Boehnert, M.U., Yeung, J.C., Bazerbachi, F., Knaak, J.M., Selzner, N., McGilvray, I.D., Rotstein, O.D., Adeyi, O.A., Kandel, S.M., Rogalla, P., et al. (2013). Normothermic acellular ex vivo liver perfusion reduces liver and bile duct injury of pig livers retrieved after cardiac death. Am. J. Transplant. *13*, 1441–1449. https://doi.org/10.1111/ajt.12224.

19. Smith, R.A.J., Hartley, R.C., Cochemé, H.M., and Murphy, M.P. (2012). Mitochondrial pharmacology. Trends Pharmacol. Sci. *33*, 341–352. https://doi.org/10.1016/j.tips.2012.03.010.

20. Murphy, M.P., and Hartley, R.C. (2018). Mitochondria as a therapeutic target for common pathologies. Nat. Rev. Drug Discov. *17*, 865–886. https://doi.org/10.1038/nrd.2018.174.

21. Liu, H., Wang, L., Weng, X., Chen, H., Du, Y., Diao, C., Chen, Z., and Liu, X. (2019). Inhibition of Brd4 alleviates renal ischemia/reperfusion injury-induced apoptosis and endoplasmic reticulum stress by blocking FoxO4-mediated oxidative stress. Redox Biol. *24*, 101195. https://doi.org/10.1016/j.redox.2019.101195.

22. Ding, M.J., Fang, H.R., Zhang, J.K., Shi, J.H., Yu, X., Wen, P.H., Wang, Z.H., Cao, S.L., Zhang, Y., Shi, X.Y., et al. (2022). E3 ubiquitin ligase ring finger protein 5 protects against hepatic ischemia reperfusion injury by mediating phosphoglycerate mutase family member 5 ubiquitination. Hepatology *76*, 94–111. https://doi.org/10.1002/hep.32226.

23. Nakamura, K., Kageyama, S., Ito, T., Hirao, H., Kadono, K., Aziz, A., Dery, K.J., Everly, M.J., Taura, K., Uemoto, S., et al. (2019). Antibiotic pretreatment alleviates liver transplant damage in mice and humans. J. Clin. Invest. *129*, 3420–3434. https://doi.org/10.1172/JCI127550.

24. Mills, E.L., Ryan, D.G., Prag, H.A., Dikovskaya, D., Menon, D., Zaslona, Z., Jedrychowski, M.P., Costa, A.S.H., Higgins, M., Hams, E., et al. (2018). Itaconate is an anti-inflammatory metabolite that activates Nrf2 via alkylation of KEAP1. Nature *556*, 113–117. https://doi.org/10.1038/nature25986.

25. Li, J., Tian, M., Hua, T., Wang, H., Yang, M., Li, W., Zhang, X., and Yuan, H. (2021). Combination of autophagy and NFE2L2/NRF2 activation as a treatment approach for neuropathic pain. Autophagy *17*, 4062–4082. https://doi.org/10.1080/15548627.2021.1900498.

26. Wu, J., Li, S., Li, C., Cui, L., Ma, J., and Hui, Y. (2021). The non-canonical effects of heme oxygenase-1, a classical fighter against oxidative stress. Redox Biol. *47*, 102170. https://doi.org/10.1016/j.redox.2021.102170.

27. Nakamura, K., Zhang, M., Kageyama, S., Ke, B., Fujii, T., Sosa, R.A., Reed, E.F., Datta, N., Zarrinpar, A., Busuttil, R.W., et al. (2017). Macrophage heme oxygenase-1-SIRT1-p53 axis regulates sterile inflammation in liver ischemia-reperfusion injury. J. Hepatol. *67*, 1232–1242. https://doi.org/10.1016/j.jhep.2017.08.010.

28. Rao, J., Qian, X., Li, G., Pan, X., Zhang, C., Zhang, F., Zhai, Y., Wang, X., and Lu, L. (2015). ATF3-mediated NRF2/HO-1 signaling regulates TLR4 innate immune responses in mouse liver ischemia/reperfusion injury. Am. J. Transplant. *15*, 76–87. https://doi.org/10.1111/ajt.12954.

29. Lin, R., Tao, R., Gao, X., Li, T., Zhou, X., Guan, K.L., Xiong, Y., and Lei, Q.Y. (2013). Acetylation stabilizes ATP-citrate lyase to promote lipid biosynthesis and tumor growth. Mol. Cell *51*, 506–518. https://doi.org/10.1016/j.molcel.2013.07.002.

30. Dey, E.S., Norrlöw, O., and Liu, Y. (2004). Artificial carrier for oxygen supply in biological systems. Appl. Microbiol. Biotechnol. *64*, 187–191. https://doi.org/10.1007/s00253-003-1454-9.

31. Kamada, N., and Calne, R.Y. (1979). Orthotopic liver transplantation in the rat. Technique using cuff for portal vein anastomosis and biliary drainage. Transplantation *28*, 47–50.

32. Ben Mosbah, I., Roselló-Catafau, J., Franco-Gou, R., Abdennebi, H.B., Saidane, D., Ramella-Virieux, S., Boillot, O., and Peralta, C. (2006). Preservation of steatotic livers in IGL-1 solution. Liver Transplant. *12*, 1215–1223. https://doi.org/10.1002/lt.20788.

33. Wu, D., and Yotnda, P. (2011). Induction and testing of hypoxia in cell culture. JoVE *54*, e2899. https://doi.org/10.3791/2899.

34. Rueden, C.T., Schindelin, J., Hiner, M.C., DeZonia, B.E., Walter, A.E., Arena, E.T., and Eliceiri, K.W. (2017). ImageJ2: ImageJ for the next generation of scientific image data. BMC Bioinf. *18*, 529. https://doi.org/10.1186/s12859-017-1934-z.

STAR★METHODS

KEY RESOURCES TABLE

REAGENT or RESOURCE	SOURCE	IDENTIFIER
Antibodies		
Mouse monoclonal anti-HSP70	Abcam	ab2787; RRID: AB_303300
Rabbit monoclonal anti-HMOX1	Abcam	ab68477; RRID: AB_11156457
Rabbit monoclonal anti-BECN1	Abcam	ab207612; RRID: AB_2692326
Mouse monoclonal anti-SIRT1	Abcam	ab110304; RRID: AB_10864359
Rabbit monoclonal anti-SIRT2	Abcam	ab211033; RRID: AB_2927614
Rabbit polyclonal anti-NFE2L2	Abcam	ab92946; RRID: AB_10561604
Rabbit polyclonal anti-eNOS	CST	Cat#32027; RRID: AB_2728756
Rabbit polyclonal anti-HSPA5	CST	Cat#3183; RRID: AB_10695864
Rabbit polyclonal anti-cleaved-CASPASE 3	CST	Cat#9661; RRID: AB_2341188
Mouse monoclonal anti-DDIT3	CST	Cat#2895; RRID: AB_2089254
Rabbit polyclonal anti-ATG5	GeneTex	GTX113309; RRID: AB_10633458
Rabbit polyclonal anti-MAP1LC3B	GeneTex	GTX127375; RRID: AB_11176277
Rabbit polyclonal anti-KHDRBS1	GeneTex	GTX100685; RRID: AB_2038029
Mouse monoclonal anti-β-ACTIN	Santa Cruz	sc-81178; RRID: AB_2223230
Chemicals, peptides, and recombinant proteins		
Polydimethylsiloxane	ZZSTANDARD	ZS-10950 CAS：8050-81-5
Poly-N-isopropyl acrylamide	Sigma-Aldrich	Cat#724823 CAS：25189-55-3
Poly[dimethylsiloxane-co-(2-(3,4-epoxy-cyclohexyl) ethyl) methylsiloxane]-copoly-N-alkyl acrylamide	This paper	Patent No (China): ZL202011044694.0
Critical commercial assays		
Flow cytometry apoptosis assay kit	4A Biotech	FXP018-100
CCK-8 assay kit	MCE	HY-K0301
MDA assay kit	Solarbio	BC0020
BCA protein assay kit	Biosharp	BL521A
Enhanced chemiluminescence kit	Millipore	WBKLS0100
TUNEL assay kit	Beyotime	C1088
ATP assay kit	Beyotime	S0026B
Experimental models: Cell lines		
LO2/HL-7702	ATCC; Oto Biotech	RRID:CVCL_6926; HTX1808
Experimental models: Organisms/strains		
Rat: Sprague-Dawley	Chengdu Dossy Experimental Animals Co., Ltd.	RRID:MGI:5651135
Software and algorithms		
SPSS 13.0	IBM Corp.	https://www.ibm.com/products/spss-statistics
GraphPad Prism 6.0	GraphPad Software Inc.	https://www.graphpad.com/scientific-software/prism/
Adobe Illustrator CS 6	Adobe Inc.	https://www.adobe.com/products/illustrator.html

(*Continued on next page*)

Continued

REAGENT or RESOURCE	SOURCE	IDENTIFIER
Quantity One 4.6.2	Bio-Rad Laboratories, Inc.	https://www.bio-rad.com/en-cn/product/quantity-one-1-d-analysis-software
Other		
Hypoxic culture chamber	Billups-Rothenberg	MIC-101
Oxygen electrode	Nuvair	O_2 Quick-Stick
UW solution	Preservation Solutions,Inc.	CoStorSol

RESOURCE AVAILABILITY

Lead contact

Further information and requests for resources and reagents should be directed to and will be fulfilled by the lead contact, Jiayin Yang (doctoryjy@scu.edu.cn).

Materials availability

The thermosensitive polymer micelles used in this study are listed in the key resources table and are available from the lead contact on request.

Data and code availability

- All data reported in this paper will be shared by the lead contact upon request.
- This article does not report the original code.
- Any additional information required to reanalyze the data reported in this article is available from the lead contact request.

EXPERIMENTAL MODEL AND SUBJECT DETAILS

Animals

Sprague-Dawley rats, male, aged 10-12wk and weighing 350-400g, were purchased from Chengdu Dossy Experimental Animals Co., Ltd. (Chengdu, China). All animals received humane care following the National Institutes of Health's Guide for the Care and Use of Laboratory Animals. All operations were approved by the Animal Care and Use Committee of West China Hospital of Sichuan University (2021130A).

Cell lines

The immortalized human liver cell line LO2/HL-7702 (hereinafter referred to as LO2), authenticated by the Chinese Academy of Sciences earlier, was cultured in high-glucose Dulbecco's modified Eagle's medium (Gibco) supplemented with 10% fetal bovine serum (BI), 100 U/mL penicillin, and 100 μg/mL streptomycin (Gibco) at 37°C in a 5% CO_2 atmosphere.

METHOD DETAILS

Development of the thermal-regulated oxygen-carrying solution

The thermal-regulated oxygen-carrying solution was based on the insight that a slow oxygen release rate is allowable for SCS due to a low metabolism rate at 4°C, but unsustainable for NMP due to considerable oxygen consumption under normothermic conditions. To achieve thermal regulation, we added to modified Krebs–Henseleit solution 4% thermosensitive polymer micelles (Poly[dimethylsiloxane-co-(2-(3,4-epoxy-cyclohexyl) ethyl) methylsiloxane]-copoly-N-alkyl acrylamide) as oxygen carrier as well as oncotic supply, hereinafter referred to as OC-KH solution for short. The thermosensitive polymer was obtained by copolymerizing polydimethylsiloxane (PDMS) and poly-N-isopropyl acrylamide (PNIPAM). PDMS is an oxophilic and biocompatible polymer in which the solubility of oxygen is 45-50 times higher than that in water.[30] However, PDMS is unable to swiftly release oxygen to meet the rising oxygen consumption as the temperature increases. Thus, we use PDMS as an oxygen-carrying segment and PNIPAM as a thermally sensitive functional segment to effectively control the oxygen release through its volume phase transition property that volume rapidly shrinks at 25°C or above to squeeze off oxygen rapidly (Figure S1A).

OCSP method

The OCSP method was an oxygen-dependent preservation strategy as it combined SCS and NMP through a common oxygen-enriched environment based on an OC-KH solution. Concretely, the liver was kept around a high-oxygen-dissolved OC-KH solution at 4°C for 24 hours, then rewarmed to 25°C gradually (taking about 1 hour), and finally followed by NMP (37°C) for 2 hours which was enough long to test liver function recovery (Figure 1). The oxygen content was reflected by the oxygen partial pressure (PaO_2) mainly determined by the physical dissolved oxygen nature of compositions in the solutions at different temperatures and also controlled by the duration and frequency of oxygen replenishment from outside (Figures S1B and S1C). We used the above thermal-regulated OC-KH solution with intermittent or successive oxygenation to yield a dynamic oxygen-enriched environment with different PaO_2 levels.

Experimental protocols

To clarify the effect of the thermosensitive polymer micelle instead of oxygen on liver preservation, we first compared the OC-KH solution and standard UW solution using SCS and OCSP methods respectively (Figures S2 andS3). Then, we focused on the potential effect on liver preservation with different PaO_2 levels as follows (Figure 1): low grade (≤200mmHg, labeled as "-") in which no oxygen replenishment from outside, medium grade (200-500mmHg, labeled as "+") in which 2.5L oxygen was fed into 30mL OC-KH solution every 20min, medium-high grade (500-650mmHg, labeled as "++") in which 5L oxygen was fed into 30mL OC-KH solution every 10min during SCS or 1L/min of oxygen was continuously fed into Krebs–Henseleit (KH) solution during NMP, and high grade (>650mmHg, labeled as "+++") in which 1L/min of oxygen was continuously fed into OC-KH solution during the whole course including SCS and NMP stage. NMP-L and NMP-H were referred to as blank control groups in which livers did not undergo the SCS process but instead went directly to NMP using KH (NMP-L group) or OC-KH (NMP-H group) solution as perfusates. The KH solution here was enriched with 5% albumin as oncotic supply with no more than 650mmHg at a maximum of PaO_2 at 37°C while the OC-KH solution could reach as high as 800 mmHg of PaO_2 at the same temperature (S-Figures S1B and S1C). Given previous studies reporting that the PaO_2 levels of UW solution were stabilized below 200 mmHg at 4°C, we set up two sequential preservation (SP) groups as the negative controls using UW solution with no oxygen supplement during SCS and rewarming phase, using KH soluting (SP-L group) or using OC-KH solution (SP-H group) as NMP perfusate. In the experimental groups, OCSP-L was referred to as relatively low content of oxygen where the highest PaO_2 levels did not exceed the medium-high grade, and OCSP-H was referred to as relatively high content of oxygen where the lowest PaO_2 levels did not fall below the medium-high grade.

After preservation, liver grafts from Sprague-Dawley rats would be transplanted in an orthotopic manner (n = 6/group) using a modified Kamada's two-cuff technique.[31] Other experiments include cell viability assay based on an IRI cell model *in vitro*, biochemical determinations, immunohistochemistry, western blots analysis, etc.

Orthotopic liver transplantation model

The donor rats were anesthetized with Zoletil 50 (5mg/100g body weight, Virbac SA, France). The livers were procured using a standard technique[32] A cross-shaped incision laparotomy was performed, and after fully freeing the liver by cutting off the ligaments around it, the abdominal aorta was cannulated, followed by slow perfusion (4mL/min) with 40mL of 0-4°C heparinized saline. Before this, 1 mL heparin normal saline (heparin concentration 125 U/mL) was injected through the subhepatic inferior vena cava to heparinize the whole body of blood. After liver removal, the grafts were preserved in UW or OC-KH solution for 24 hours at 4°C, in an oxygen-enriched or low-oxygen environment as the above protocols described. Thereafter, livers were submitted to 2 hours of NMP following rewarming, using an isolated perfused rat liver model, as described elsewhere[4]

After preservation, liver grafts would be transplanted in an orthotopic manner (n = 6/group) using a modified Kamada's two-cuff technique.[31] The recipient rats were anesthetized with continuous inhalation of ether as well as intramuscular injection of atropine 0.03mg/kg which counteracted the increase in respiratory secretions caused by ether and thus prevented aspiration. In transplantation, the portal vein and inferior hepatic vena cava were anastomosed with their respective namesake veins using the two-cuff approach. The superior hepatic vena cava were sutured with suture lines, and the bile duct was reconstructed in a stent implantation way. After transplantation, the rats were moved to the vicinity of a heater and rewarmed for two hours followed by giving 5% dextrose saline, and given a diet one day later.

All procedures were approved by the Animal Care and Use Committee of West China Hospital of Sichuan University.

In vitro IRI cell model

A modified *in vitro* IRI cell model was established via the modular incubator chamber method.[33] Briefly, The adherent cells immersed in the preservation solution to be tested were placed in the hypoxic culture chamber (MIC-101, Billups-Rothenberg) at 4°C for 24 hours or 48 hours to simulate the process of cold ischemia, and the hypoxic environment with no more than 1% oxygen concentration detected by oxygen electrode (O_2 Quick-Stick, Nuvair) was maintained by precharge and subsequent nitrogen (N_2) filling. Then, the cells were transferred back to the complete cell culture medium preheated to 37°C followed by culturing in the conventional cell incubator for 6 hours to simulate the process of reperfusion after ischemia (Figure S4A). After the established model, cell morphology was observed by inverted microscope (OBSERVER D1/AX10 cam HRC, Zeiss) and hematoxylin and eosin (HE) staining of cell slides before reperfusion and cell activity was detected by flow cytometry apoptosis detection kit (FXP018-100, 4A Biotech) as well as by cell counting kit-8 (CCK-8, HY-K0301, MCE) after reperfusion.

Biochemical determinations

Liver injury was assessed according to transaminase levels in effluent perfusates as well as in solutions at the end of cold preservation as baseline level with an automatic biochemical analyzer (BS-240, Mindray). Liver function was assessed by measuring cumulative bile production and the output was reported as ul/min/g liver. Lipid peroxidation was determined by measuring the formation of malondialdehyde (MDA) with a thiobarbituric acid method in strict accordance with the commercial kit (BC0020, Solarbio) instructions.

Immunohistochemistry

Liver tissues were taken and fixed immediately at the end of preservation/perfusion. After dehydration, transparency, wax immersion, embedding and slicing, they were made into sections and stored at room temperature. Before the experiment, liver sections were dried in an oven at 65°C overnight, and then dewaxing, hydration, antigen repair, permeabilization, blocking, and antibody incubation were performed in turn. The primary antibody (anti-HSP70, mouse monoclonal Ig, Abcam; anti-eNOS, rabbit polyclonal IgG, CST; or anti- HMOX1, rabbit monoclonal, Abcam) was applied at a dilution of 1:200 in the blocking solution and incubated at 4°C overnight. After rinsing in double-distilled water and wash buffer, the secondary antibody (Alexa Fluor 488 labeled, goat anti-rabbit, or goat anti-mouse, CST) was applied at the dilution of 1:200 in the blocking solution for 1 hour at 37°C. After the secondary antibody incubation, DAPI working solution (Invitrogen) was added to stain the nucleus and incubated for 3-5min. Images were obtained with a Leica DM2500 fluorescence microscope.

Western blots analysis

Proteins from liver tissues were extracted using RIPA buffer (containing 1% phenylmethylsulfonyl fluoride and 1% phosphatase inhibitors). The BCA protein assay kit (BL521A, Biosharp) was used to determine the protein concentration. Proteins were separated by SDS-PAGE and transferred into polyvinylidene fluoride (PVDF) membranes. The PVDF membranes were blocked with 5% non-fat dried milk in tris-buffered saline (pH 7.4) containing 0.1% Tween20 and subsequently immunoblotted with antibodies directed against BECN1 (ab207612, Abcam), ATG5 (GTX113309, GeneTex), MAP1LC3B (GTX127375, GeneTex), KHDRBS1 (GTX100685, GeneTex), HSPA5 (#3183, CST), DDIT3 (#2895, CST), SIRT1 (ab110304, Abcam), SIRT2 (ab211033, Abcam), NFE2L2(ab92946, Abcam), HMOX1 (ab68477, Abcam), cleaved-CASPASE 3 (#9661, CST), and β-ACTIN (sc-81178, Santa Cruz). The bands were visualized via an enhanced chemiluminescence kit (WBKLS0100, Millipore) and the semi-quantitative analysis was conducted by the Quantity One software program (Bio-Rad).

Histology

Liver tissues were fixed in 10% formalin. After embedding, samples were sectioned and stained with HE. After staining, three pathologists would respectively be assigned a semiquantitative score to evaluate hepatocyte injury and then took the average value. Biopsy tissue was examined for cell swelling (0, absent; 1, mild/< 30%; 2, moderate/30-60%; 3, severe/> 60%) and necrosis (0, absent; 1, mild/< 30%; 2, moderate/30-60%; 3, severe/> 60%) in a blinded fashion.

Electron microscopy

Liver tissues of the appropriate size (1mm^3) were freshly obtained and immediately fixed in a mixture of 2.5% glutaraldehyde and 4% paraformaldehyde. After dehydration in an ethanol gradient, samples were embedded and sectioned. Electron microscopy was performed using a transmission electron microscope (JEM1230, JEOL) at 100kV, and images were recorded with a digital camera.

Terminal deoxynucleotidyl transferase-mediated dUTP nick end-labeling (TUNEL) assay

According to the manufacturer's instructions, TUNEL was performed with the commercial kit (C1088, Beyotime). Briefly, liver tissue sections were deparaffinized and incubated with terminal deoxynucleotidyl transferase in a humidifier chamber at 37°C for 1 hour. Apoptosis was observed under the fluorescence microscope and images were recorded, in which strong green fluorescence in the nucleus indicated a positive cell. i.e. apoptotic cell. Each slice was selected with 3 high magnification views, and the percentage of apoptosis (%) was calculated using ImageJ professional image analysis program.[34]

ATP assay

Liver tissues were taken for ATP content measure at 0.5-, 1-, 2-, 4-, 6-, 8-, 12-, 24-, 25-, 26-, and 27-hour during preservation using a firefly luciferase-based assay kit (Beyotime Inc.). ATP content was normalized to protein content which was measured with a Bradford protein assay kit (Beyotime Inc.) and was expressed as pMoles/mg protein.

QUANTIFICATION AND STATISTICAL ANALYSIS

All statistical analyses were performed using SPSS 13.0 (IBM Corp.), and figures were produced using GraphPad Prism 6.0, or Adobe Illustrator CS 6. Data are expressed as mean +/- SD from at least three independent experiments unless otherwise noted. Comparisons between two groups were performed by two-tailed Student t-test or multiple groups by one-way analysis of variance (ANOVA). Survival was evaluated by the log-rank test. Statistical significance was considered if $P < 0.05$.

ADDITIONAL RESOURCES

This article does not report additional websites or resources.